STRUCTURE OF MATTER
AND QUANTUM CHEMISTRY

Changes in the Crystal Lattice Parameters of Montmorillonite during Its Modification by Cobalt and Aluminum Cations

P. V. Sokolovskiy[a],*, F. Roessner[b],**, A. I. Vezentsev[c],***, T. V. Konkova[d], M. B. Alekhina[d],****,
S. S. Manokhin[e],*****, and A. A. Greish[a]

[a]Zelinsky Institute of Organic Chemistry, Russian Academy of Sciences, Moscow, 119991 Russia
[b]Ossietzky University of Oldenburg, Oldenburg, 26129 Germany
[c]Belgorod National State Research University, Belgorod, 308015 Russia
[d]Mendeleev University of Chemical Technology of Russia, Moscow, 125047 Russia
[e]Institute of Problems of Chemical Physics of the Russian Academy of Sciences, Moscow, 142432 Russia
*e-mail: carbsorb@gmail.com
**e-mail: frank.roessner@uni-oldenburg.de
***e-mail: vesentsev@bsu.edu.ru
****e-mail: mbalekhina@yandex.ru
*****e-mail: manohin@bk.ru

Abstract—The effect the modification (pillarization) of montmorillonite clays from different locations has on the crystallographic lattice parameters of montmorillonite is determined. It is revealed through ultrahigh resolution transmission electron microscopy and analyzing microdiffraction patterns that pillarization raises the distance between montmorillonite structural units to 2.2 nm, while the intracrystal distance between the atoms grows by 0.4 nm. The catalytic activity of specimens in the oxidation reaction between organic dyes and hydrogen peroxide is enhanced 2–3 times.

INTRODUCTION

The environment is nowadays being polluted everywhere by discharges of industrial waste water. Discharges are often highly toxic and are difficult to extract from water. The most efficient way of cleaning waste water is catalytic oxidation in the presence of hydrogen peroxide [1]. During the interaction between hydrogen peroxide and transition metal ions, active hydroxyl radicals form in a solution [1] and initiate radical chain reactions that result in the oxidation of organic compounds. Due to their low cost and the possibility of forming stable pillars, pillared clays containing transition metal ions are promising carriers for catalysts used at sewage treatment plants [1]. The preparation of structures of this type offers wide opportunities for using pillared clays as catalysts in redox processes, particularly the catalytic destruction of organic impurities in waste water. Hybrid and other nanomaterials on have been widely used in catalytic purification [2–12]. Montmorillonite clays are also nanomaterials. Studying the structural changes that occur inside the montmorillonite crystal lattice during the formation of a pillared structure is an important task associated with the

pillarization mechanism at the atomic level. By changing the interlayer distances in montmorillonite crystals, we can alter the crystal structure of pillared clays, depending on their function in the catalytic destruction of organic impurities in waste water.

Al and Al—Fe montmorillonite clays are the ones most abundant in sedimentary strata, while weathering rinds and hydrothermally altered soils most often contain nontronite (Fe-montmorilonite), saponite (Mg-montmorrilonite), hectorite (Li—Mg montmorrilonite), and Ca montmorillonite clays [13]. Montmorilonite clays are characterized by their ability to swell, especially if there are Na^+ cations on exchange sites. Montmorrilonite minerals are found in nature as fine, often nanosized, imperfect crystals. A layered Al-montmorillonite unit (Fig. 1) consists of two outer tetrahedral silicon-oxygen networks and one octahedral aluminum-oxygen network between them.

The vertices of silicon-oxygen tetrahedra occupied by oxygen ions of both marginal tetrahedral layers are directed toward the middle octahedral layer. There, oxygen ions are bonded to such trivalent cations as aluminum, magnesium, iron, and other metal ions
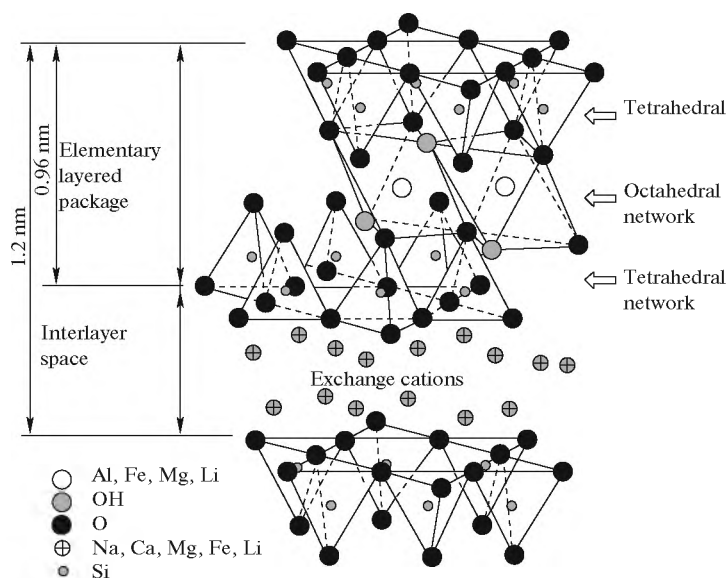
Fig. 1. Scheme of the montmorillonite crystal lattice [19].

six-coordinated in the central layer. Montmorillonite unit layers are spaced 0.96 nm from one another and are linked by weak Van der Waals forces. The montmorillonite unit layers are continuous in directions x, y and ordered relative to one another in direction z. The distance between the units is 0.24 nm [14–19].

According to the data in [20, 21], up to 15% of the tetrahedral layer of montmorillonite can consist of isomorphic Al^{3+} substitutions. As a result of these substitutions, excess negative charge appears because of a reduction in the positive charge, and the crystal lattice becomes electrically unbalanced. The charge is neutralized only by exchange cations located between the structural layers [13]. The structural features of montmorillonite allow us to measure interplanar distances by introducing exchange cations into the interunit space, which can in turn affect the sorption characteristics of montmorillonite with respect to large organic molecules.

One promising way of modifying the crystal lattice of montmorillonite to increase interplanar distances is pillarization. Clay is submerged into a pillaring solution containing poly(hydroxometal) cations to accomplish the ion exchange of interlayer clay cations with polyhydroxy cations of different nature (e.g., Al^{3+}, Fe^{3+}, Ti^{4+}, Zr^{4+}). Subsequent thermal treatment of the material is accompanied by dehydroxylation of the introduced polyhydroxy cations, as a result of which metal oxide clusters (columns or pillars) form in the interlayer space of montmorillonite that are strongly bound to the layers of alumosilicate clay by oxygen bridges. Clays subjected to this modification are referred to as pillared [22, 23].

The aim of this work was to synthesize cobalt-containing pillared clays and study the crystallographic lattice parameters of montmorillonite. We therefore obtained experimental specimens modified by a pillar-

ing solution containing Co^{2+} cations. Introducing clays of transition metal ions (Co^{2+}) into the interlayer space, which can experience reversible redox transformations, allows their application in heterogeneous catalysis, particularly the oxidative destruction of organic compounds in waste water by hydrogen peroxide (the Fenton process) [22].

EXPERIMENTAL

Specimens of montmorillonite-containing clays from the Polyana field (Belgorod oblast, Russia) with montmorillonite concentrations of 48–62 wt % and the Tagan deposit (Kazakhstan) with montmorillonite concentrations of 90–95 wt % were used as our initial materials. The clay specimens were modified by treating them with a pillaring solution containing Al^{3+} and Co^{2+} in a 9 : 1 mole ratio, with subsequent thermal treatment (annealing temperature, 500°C). Systems based on an aqueous solution of a mixture of aluminum and cobalt nitrates with mole ratio $Al^{3+} : Co^{2+} = 9 : 1$ and a total molar concentration of 0.2 mol/L of the above metal ions were chosen as pillaring solutions. The joint hydrolysis of aluminum and cobalt ions was performed with sodium hydroxide at 60°C, a 0.2 M concentration of the solutions, $OH^- : Me_n^+ = 2 : 1$. After holding the complex for 7 days, the ion exchange stage was conducted at 60°C. The precipitate was then washed via decantation, dried at room temperature, and annealed at 500°C for 2 h. The procedure for modifying montmorrilonite clay was described in detail in [22]. The clay specimens were referred to as P_{in} and P_{mod} (the initial and modified clay specimens of the Polyana field) and T_{in} and T_{mod} (the initial and modified clay specimens of the Tagan Deposit).

The elemental composition of the clay specimens was determined through X-ray fluorescence using the X-MAX INCA ENERGY attachment (Oxford Instruments, Great Britain) on the JEOL JSM-6510 LV (JEOL, Japan) electron microscope at the Shared Resource Center of Mendeleev University of Chemical Technology of Russia. The results from analyzing the initial and modified clays are summarized in Table 1.

Our experiments showed that after the initial clay specimens were modified, Co appeared in the chemical composition of pillared specimens in concentrations of 0.26 and 0.39 wt % (specimens P_{mod} and T_{mod}, respectively). A drop in the concentrations of Ca, Na, and Mg was also observed in the modified specimens; these were transferred to the solution as a result of ion exchange.

The morphological characteristics and crystallographic parameters of the native and modified montmorillonite were determined using a Technai G2F20 S-Twin (FEI Company, the Netherlands) high-resolution field emission transmission electron microscope. To study montmorrilonite clays, we prepared specimens and suspensions that were not self-sustaining [24, 25]. A carbon film obtained by depositing spectrally pure carbon on the surface of a single halite crystal was used as a substrate. Immediately before deposition, the halite crystal was split along the planes of cleavage to obtain a clean, smooth surface. Deposition was performed using the universal Quarum Q150RE vacuum system. Pulses at pressures of 4–10 mBar (2 to 4 pulses for 2–5 s at 30 s intervals) were used in this procedure. To separate the carbon film from the halite surface, a fragment of the split single halite crystal with the deposited film was placed on the surface of distilled water poured into a low, flat crystallizer with a large free surface area. The halite crystal dissolved, and the carbon film floated on the water's

Table 1. Chemical composition of our experimental clay specimens (wt %)

Specimen	Si	Al	Ca	Na	Mg	K	Fe	Co
P_{in}	24.98	8.89	0.56	0.32	1.17	2.28	3.39	—
P_{mod}	15.16	8.20	0.03	0.07	0.83	1.20	2.22	0.26
T_{in}	23.64	7.62	0.86	0.85	1.56	—	3.10	—
T_{mod}	13.85	9.33	0.05	0.14	1.03	—	1.77	0.39

surface. A pre-cleaned copper grid was secured with clamps and the carbon film was caught to cover the grid.

A drop of an aqueous suspension of the investigated specimen was applied to the dried grid with the carbon film on it. To minimize the statistical error, the specimens were analyzed using three grids with a specimen deposited from the same sample after thorough stirring of the same sample before each deposition on the grid [26]. A laboratory sample was formed by isolating part of the middle sample of the specimen in an amount sufficient to perform a single analysis [27]. Microdiffraction of electrons from the selected region in the point electron diffraction mode was employed to identify minerals [28].

RESULTS AND DISCUSSION

In analyzing the microstructure of initial montmorilonite clay from the Polyana field (P_{in}), it was found the montmorillonite consisted of isometric cloud-like nanofilmed crystals 2–3 nm thick (Fig. 2). A similar morphology of montmorillonite crystals was observed in [28]. The microdiffraction pattern of montmorillonite crystals is typically in the form of concentric
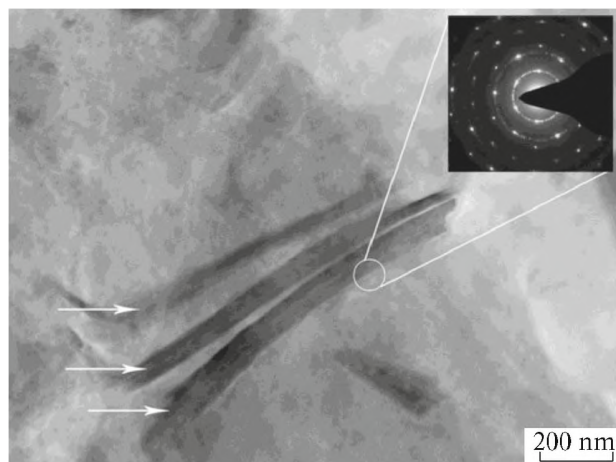

Fig. 2. Separate montmorillonite crystals (marked with arrows) in specimen P_{in} (the electron microdiffraction pattern is shown in the upper right corner).
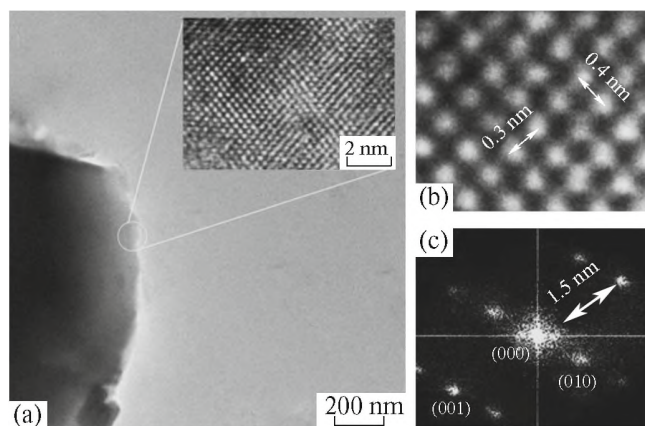

Fig. 3. Light field image of a montmorillonite crystal from specimen P_{in} (a) (an ultra-high resolution photo of the crystal lattice of a single montmorillonite crystal is shown in the upper right corner); (b) magnified region of an ultra-high resolution measurement of the crystal lattice of a single montmorillonite crystal; (c) Fourier electron diffraction pattern of the region of measurement.
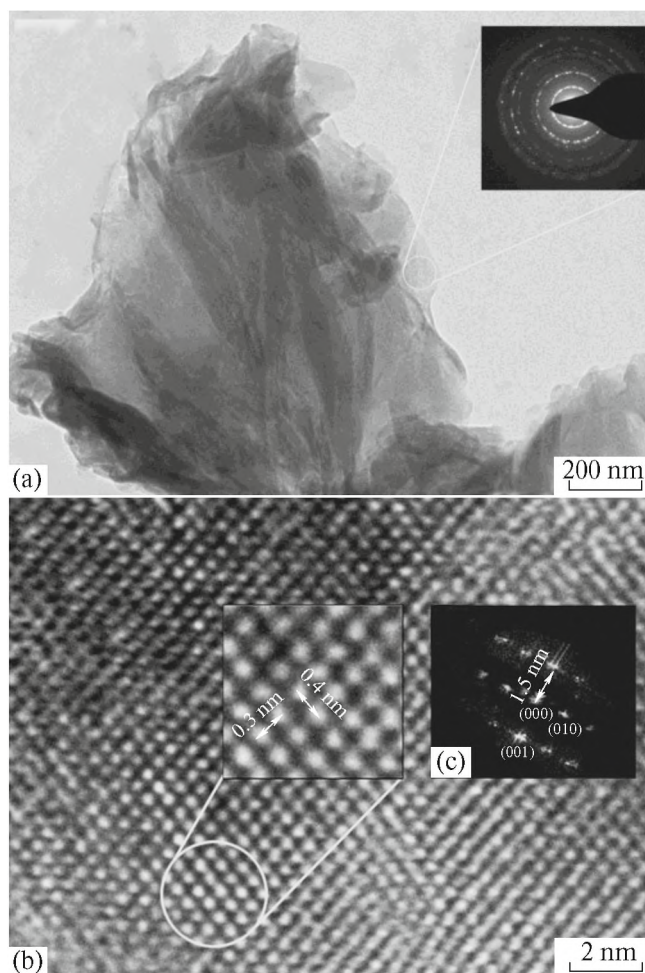
Fig. 5. (a) Light field image of a montmorillonite crystal from specimen P_{mod} (an ultra-high resolution photo of the crystal lattice of a montmorillonite single crystal is shown in the upper right corner); (b) magnified region of an ultra-high resolution measurement of the crystal lattice of a single montmorillonite crystal; (c) Fourier electron diffraction pattern of the region of measurement.

Fig. 4. (a) Light field image of a montmorillonite crystal from specimen T_{in} (the electron microdiffraction pattern is shown in the upper right corner); (b) ultra-high resolution photo of the crystal lattice of a single montmorillonite crystal; (c) Fourier electron diffraction pattern of the region of measurement.

Fig. 6. (a) Light field image of a montmorillonite crystal from specimen T_{mod} (an ultra-high resolution photo of the crystal lattice of a single montmorillonite crystal is shown in the upper right corner); (b) magnified region of an ultra-high resolution measurement of the crystal lattice of a single montmorillonite crystal; (c) Fourier electron diffraction pattern of the region of measurement.

rings (Fig. 2) [28]. This structure corresponds to a layered silicate of the 2 : 1 structural type with a swelling (montmorillonite) crystal lattice, according to the X-ray data of ASTM International [29]. Based on our calculations, this crystal belongs to symmetry group P and has a monoclinic crystal lattice with lattice parameters $a = 5.29$ Å, $b = 9.19$ Å, $c = 15.49$ Å, which is fully consistent with the literature data [30].

Light field analysis of the specimen P_{in} (Fig. 3) allowed us direct resolution of a filmed single (nanodisperse) montmorillonite crystal (Fig. 3a). The intracrystal distances were 0.3 and 0.4 nm (Fig. 3b). The Fourier electron diffraction pattern allowed determination of the interpackage distance at the atomic level. Analysis showed that the montmorillonite crystal from specimen P_{in} had an interpackage distance of 1.5 nm along axis (001), which corresponds to montmorillonite with a monoclinic crystal lattice (Fig. 3c).
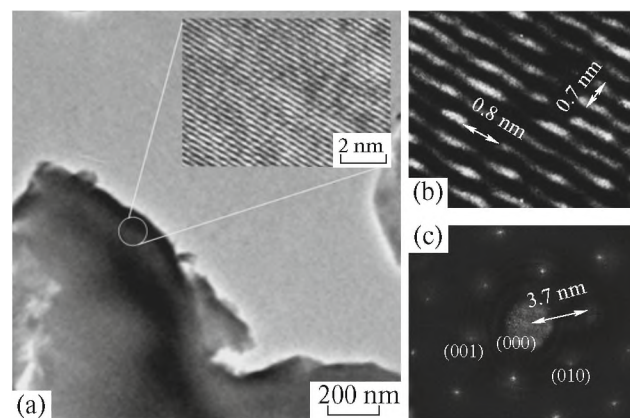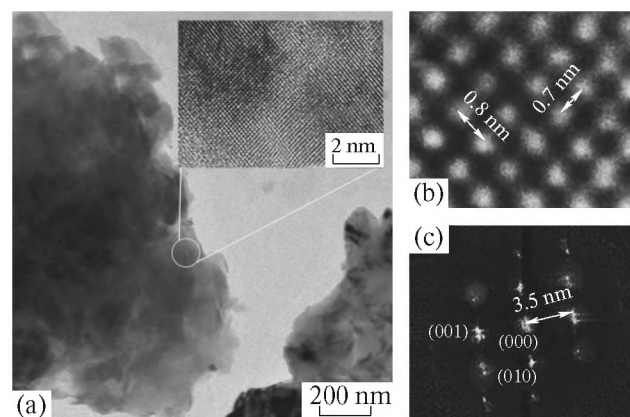
The crystal structure of montmorillonite from specimen P_{in} was compared to that of the montmorillonite in the composition of specimen T_{in}. It was found that the montmorillonite crystals in specimen T_{in} were also in a cloud-like nanofilmed form (Fig. 4a) and the microelectron pattern typical of montmorillonite (Fig. 4a).

The light field image and the high-resolution electron images of montmorillonite clay from the Tagan deposit did not differ appreciably from those of the Polyana field (Fig. 4). The intracrystal distances were 0.3 and 0.4 nm (Fig. 4b), and the interpackage distance along axis (001) was 1.5 nm (Fig. 4c).

Our light field study of modified clay specimen P_{mod} (Fig. 5a) demonstrated the effectiveness of the

pillaring technique to form a pillared structure of clays. The direct resolution of this specimen (Fig. 5a) allowed determination of the intracrystal distances, which grew by 0.4 nm relative to those in the initial specimen of P_{in} (Fig. 3c) and were 0.7 and 0.8 nm (Fig. 5b). The interpackage distance along axis c (001) grew by 2.2 nm, reaching 3.7 nm (Fig. 5c).

The light field study of specimen T_{mod} yielded similar results (Fig. 6). The intracrystal distances were 0.7

and 0.8 nm (Fig. 6b), while the interpackage distance along the c(001) axis was 3.5 nm (Fig. 6c).

The sorption characteristics of the initial and modified clay specimens with respect to azorubine (an anionic dye) and methylene blue (a cationic dye) organic dyes were determined in the range of low concentrations [23]. Below, we present the structural formulas of (a) azorubine and (b) methylene blue:

(a)

(b)
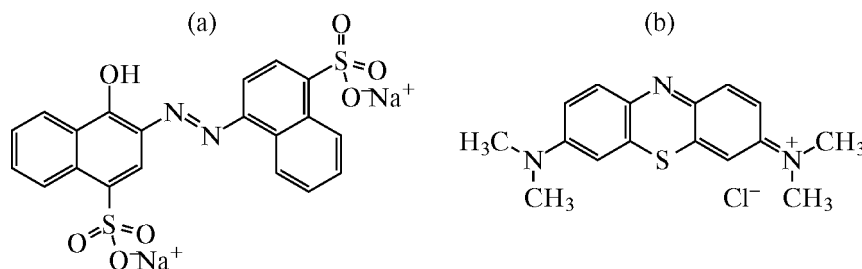
The results from our study are summarized in Table 2, which also lists the data from measuring the electrokinetic potentials of these specimens in an aqueous solution, obtained via electrophoresis on a ZetasizerNano unit (MALVERN Instruments, Great Britain).

Our experiments revealed the pillarization of Polyana clay increased its sorption capacity by 1.6 times with respect to azorubine (an anionic dye). The adsorption capacity of a pillared specimen of Tagan clay with respect to azorubine remained at the capacity level of the initial specimen. It was found the sorption capacity of both initial and pillared clays with respect to methylene blue was several times higher than the one with respect to azorubine at the same initial concentrations of the dyes in the solution. The adsorption capacities of both initial and pillared clays with respect to methylene blue were virtually identical.

We assume the different adsorptivity of the cationic and anionic dyes on the studied specimens to be due primarily to different charges on the surfaces of clay

specimens. As is seen from Table 2, the electrokinetic potential of specimen T_{in} was twice that of specimen P_{in}. After pillarization, the surface charges of the clay specimens remained virtually the same.

Montmorrilonite clays can thus be recommended as adsorbents to cleanse waste water, mainly of cationic dyes.

Table 3 lists the results from the catalytic destruction of carmoisine with hydrogen peroxide in the presence of both initial and pillared clay specimens from the Polyana field and the Tagan deposit. The structural formula of carmoisine is
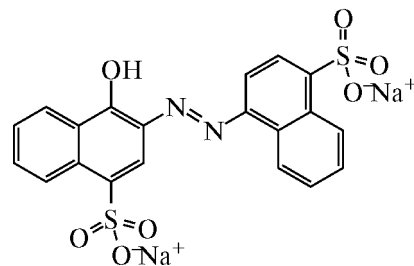
The specific surface values were calculated using the BET equation, based on isotherms of nitrogen adsorption at 77 K, measured on a Nova 1200e apparatus (Quantachrome).

As is seen from Table 3, the modifying of natural montmorrilonite clays increased the specific surfaces of specimens and consideraly enhanced their catalytic activities: the degree of dye (carmoisine) transformation on the modified specimens rose 2–3 times, compared to the one on the initial specimens.

Table 2. Adsorption capacity of clays with respect to organic dyes: azorubine and methylene blue (initial concentration of dyes in the solution was 10 mg/L)

Specimen	A, mg/g		$-\zeta$, mV
	with respect to azorubine	with respect to methylene blue	
P_{in}	0.16	1.05	25.6
P_{mod}	0.26	1.18	22.9
T_{in}	0.05	1.17	47.0
T_{mod}	0.07	1.18	46.4

ζ is the electrokinetic potential; A is the adsorption capacity of the specimen.

CONCLUSIONS

Our data show that modifying montmorillonite using pillaring solutions based on aqueous solutions of

Table 3. Catalytic destruction of carmoisine with hydrogen peroxide in the presence of initial and pillared clay specimens from the Polyana and Tagan deposits

Catalyst specimen	S_{sp} according to BET, m^2/g	Degree of carmoisine transformation, %
P_{in}	64	50
P_{mod}	84	99
T_{in}	66	33
T_{mod}	101	96

Carmoisine concentration, 20 mg/L; double excess of peroxide; temperature 60°C; pH 3.

a mixture of aluminum and cobalt nitrates with mole ratio $Al^{3+}:Co^{2+} = 9:1$ and a total molar concentration of metal ions of 0.2 mol/L with subsequent annealing at 500°C is an effective way of increasing the interplanar distance in the montmorillonite crystal lattice. It was shown via TEM that the proposed modification procedure results in a 2.2 nm increase in the distance between the montmorillonite packages, and to a 0.4 nm increase in the intracrystal distance. The obtained pillared clays can be used for the adsorption cleansing of cationic dyes and heterogeneous catalysis, particularly the oxidative destruction of organic compounds in waste waters with the use of hydrogen peroxide (the Fenton process).

ACKNOWLEDGMENTS

REFERENCES

1. T. V. Kon'kova, M. B. Alekhina, M. V. Papkova, et al., Ekol. Prom-st' Ross., No. 3, 32 (2013).
2. A. V. Kirilin, A. V. Tokarev, L. M. Kustov, et al., Appl. Catal., A **435–436**, 172 (2012).
3. V. P. Ananikov, E. G. Gordeev, M. P. Egorov, et al., Mendeleev Commun. **26**, 365 (2016).
4. V. P. Ananikov, D. B. Eremin, S. A. Yakukhnov, et al., Mendeleev Commun. **27**, 425 (2017).
5. A. V. Tokarev, E. V. Murzina, J.-P. Mikkola, et al., Chem. Eng. J. **134**, 153 (2007).
6. L. M. Kustov, E. D. Finashina, E. V. Shuvalova, et al., Environ. Int. **37**, 1044 (2011).
7. A. Yu. Khodakov, C. Williams, L. M. Kustov, et al., J. Chem. Soc., Faraday Trans. **89**, 1393 (1993).
8. V. P. Ananikov, K. I. Galkin, M. P. Egorov, et al., Mendeleev Commun. **26**, 365 (2016).
9. V. P. Ananikov, ACS Catal. **5**, 1964 (2015).
10. K. S. Egorova and V. P. Ananikov, Angew. Chem., Int. Ed. Engl. **55**, 12150 (2016).
11. D. B. Eremin and V. P. Ananikov, Coord. Chem. Rev. **346**, 2 (2017).
12. V. I. Bukhtiyarov, V. I. Zaikovskii, A. S. Kashin, et al., Russ. Chem. Rev. **85**, 1198 (2016).
13. B. Velde, Clay Miner. **36**, 271 (2001).
14. T. Cheng-Che, Y. Juang, S. A. Dai, et al., J. Mater. Chem. **16**, 2056 (2006).
15. E. G. Kukovskii, *Specific Features of the Structure and Physicochemical Properties of Clay Minerals* (Naukova Dumka, Kiev, 1966) [in Russian].
16. T. Grygar, D. Hradil, P. Bezdieka, et al., Clays Clay Miner. **55**, 165 (2007).
17. A. Robert, Clay Clay Miner. **50**, 411 (2007).
18. S. W. Bailey, Am. Mineralog. **65**, 11 (1980).
19. Yu. K. Egorov-Tismenko, *Crystallography and Crystal Chemistry* (KDU, Moscow, 2005) [in Russian].
20. V. N. Sokolov, Soros. Obrazov. Zh., No. 9, 59 (1996).
21. Ch. Poole and F. Owens, *Introduction to Nanotechnology* (Wiley, Hoboken, NJ, 2003; Tekhnosfera, Moscow, 2004).
22. T. V. Kon'kova, M. B. Alekhina, and A. P. Rysev, Russ. J. Phys. Chem. A **87**, 1762 (2013).
23. T. V. Konkova, M. B. Alekhina, and A. I. Mikhailichenko, Prot. Met. Phys. Chem. Surf. **50**, 326 (2014).
24. *Electron Microscopy of Thin Crystals,* Ed. by P. B. Hirsch, A. Howie, R. B. Nicholson, D. W. Pashley, and M. J. Whelan (Plenum Press, New York, 1965; Mir, Moscow, 1968).
25. D. Shindo and T. Oikawa, *Analytical Electron Microscopy for Materials Science* (Springer, Japan, 2002; Tekhnosfera, Moscow, 2006).
26. MR (Guidelines) No. 1.2.2641-10 (2010).
27. MR (Guidelines) No. 1.2.0022-11 (2011).
28. K. Müller and K. Gries, *Advanced Methods in Transmission Electron Microscopy, TEM Tutorial Riezlern* (Inst. Festkorperphys. Bereich Elektronen mikroskopie, Univ. Bremen, 2008).
29. *Complete 82-Volume Set of ASTM Standards* (ASTM, West Conshohocken, 2011).
30. H.-M. Thao, Doctoral Dissertation (Facult. Math. Nat. Sci., Ernst-Moritz-Arndt-Univ., Greifswald, Germany, 2006).

Translated by L. Chernikova